

## **A Paleoclimate Reconstruction Based on a Biogenic Oxalate Rock Crust**

Jon Russ,\* David H. Loyd and Thomas W. Boutton

A calcium oxalate rock crust that occurs in southwestern Texas was produced by an epilithic lichen that flourished during dry climate conditions. During wet climate regimes the vitality of the organism was severely reduced, decreasing or terminating the production of calcium oxalate. Thus, the vitality of the lichen—and the production of calcium oxalate—waxed and waned in response to wet–dry climate fluctuations. A paleoclimate reconstruction based on 25 oxalate AMS radiocarbon ages demonstrates the region experienced wet–dry climate episodes that coincides with global climate trends, including dry conditions during the Holocene Climate Optimum and Medieval Warm Period, and wet conditions during the Little Ice Age.

---

Variations in global climate appear to have become more complex during the mid and late Holocene (1), which increases the difficulty of resolving the mechanisms of short-term (decadal/centennial scale) climate fluctuations and predicting near future climate changes due to anthropogenic greenhouse gas emissions. To discriminate between potential mechanisms of short-term climate fluctuations (2) superimposed on modifications due to orbital variations (3) will require new sources of high resolution paleoclimate data. We recently suggested that a

---

J. Russ, Department of Chemistry and Physics, State University, AR 72467.

D. H. Loyd, Department of Physics, Angelo State University, San Angelo, TX 76909.

T. W. Boutton, Department of Rangeland Ecology and Management, Texas A&M University, College Station, TX 77843.

---

\*To whom correspondence should be addressed.

calcium oxalate rock crust produced by past lichen activity on limestone surfaces in southwestern Texas can serve as a paleoenvironmental proxy (4). Presented here is a paleoclimate reconstruction based on this biogenic residue.

Calcium oxalate (whewellite,  $\text{CaC}_2\text{O}_4 \cdot \text{H}_2\text{O}$ ) occurs as a thin (usually  $\leq 0.5$  mm but up to 1.0 mm thick), ubiquitous coating on limestone surfaces inside dry rock shelters and under rock overhangs throughout the canyons of the southern Edwards Plateau of Texas (5). The oxalate was produced by an epilithic lichen, tentatively identified as *Aspicilia calcarea*, as established by morphological and biochemical similarities between the rock crust and recent lichen residues found in two sites (4). Gypsum ( $\text{CaSO}_4 \cdot 2\text{H}_2\text{O}$ ) is a secondary crust constituent that occurs within microfissures in the crust and substrate, and occasionally as independent crust strata. The gypsum was produced by efflorescence, that is, precipitation of calcium sulphate from water saturated with the ions percolating through the substrate and evaporating at the surface. Silicates comprise a minor crust component, likely from eolian matter adhering to the surfaces when damp from dew or fog (6), while quartz and silicates native to the substrate are distributed heterogeneously within the basal limestone.

The ubiquity of oxalate on limestone surfaces not exposed to rain or runoff indicates the lichen flourished in these niches. We suggest the maximum vitality of the organism occurred during dry climate conditions, specifically when evaporation exceeded precipitation (high E:P) that reduced the moisture content of the Edwards limestone platform. The dry rock surfaces would provide the ideal substrate on which the lichen would thrive by allowing the organism to obtain requisite moisture via water vapor uptake, the most efficient mechanism for some xeric lichen species (7). During periods of low E:P the increased moisture content of the limestone plateau would reduce the vitality of the lichen due to a variety of possible physiological responses,

including blockage of CO<sub>2</sub> diffusion pathways in the thallus (6), a water imbalance that severely limits either the fungal or algal components of the lichen, or response to freezing water (8). Moreover, since substrate water would be saturated with calcium and sulfate ions, evident by the presence of gypsum in the crust, the pH or ionic environment might also be deleterious to the lichen. Hence, the vitality of the lichen—and the production of calcium oxalate—waxed and waned in response to dry-wet climate fluctuations.

We established a record of past lichen activity based on radiocarbon ages of oxalate collected from sites along the Rio Grande, Pecos River, Devils River, and adjacent dry canyon tributaries (5). Samples that showed evidence of recent biological activity or the potential of multiple periods of oxalate deposition observed using optical microscopy and SEM were excluded from the study; however, two samples with well defined oxalate/gypsum stratification were selected for <sup>14</sup>C dating, with the upper and lower strata removed and dated separately.

Samples were prepared for AMS <sup>14</sup>C dating by removing loose detritus from the surface by light scrubbing with deionized water. The oxalate crust was removed from the limestone substrate using a dental pick or minidrill, ground using an agate mortar and pestle, then digested in 5% double distilled acetic acid or dilute phosphoric acid to remove carbonates (9). Samples were washed, filtered and dried, then combusted at 950°C in the presence of CuO to produce CO<sub>2</sub>. Graphite targets were prepared using standard protocol for the AMS radiocarbon analysis (10). When sufficient sample remained, a second aliquot was converted to CO<sub>2</sub> and the stable carbon isotope ratio (δ<sup>13</sup>C<sub>PDB</sub>) measured by isotope ratio mass spectrometry (4).

A paleoclimate record is presented here based on 25 AMS <sup>14</sup>C radiocarbon ages of oxalate samples collected from 14 sites (Table 1, Fig. 1). Clusters of <sup>14</sup>C dates correspond to periods of high lichen productivity and thus episodes of high E:P; gaps in the data indicate periods of low

E:P when the lichen was absent or dormant. Accordingly, four xeric episodes are recorded for the late and mid Holocene: from 680 to 1360 cal yr BP (X1), from 1760 to 2080 cal yr BP (X2), from 2840 to 5020 cal yr BP (X3), and from 6030 to 6380 cal yr BP (X4). Wet conditions occurred from present to 680 cal yr BP (M1), from 1360 to 1760 cal yr BP (M2), from 2080 to 2840 cal yr BP (M3), and from 5020 to 6030 cal yr BP (M4). The paucity of  $^{14}\text{C}$  data older than about 6380 cal yr BP limits predicting earlier climate regimes.

Previous paleoclimate reconstructions for the southern Edwards Plateau based on palynological, plant macrofossil, and vertebrate fossil data indicate the region experienced a general decrease in effective moisture beginning at the end of the Pleistocene, with xerophytic plant species becoming present ~7000 yr BP (11, 12). The driest interval occurred between 5000–2500 yr BP (12), followed by a return to mesic conditions ca. 2500 yr BP. However, Bryant and Holloway (11) describe this mesic interval as brief, while Toomey *et al.* (12) suggest an extended period of relatively high moisture, possibly until ca. 1000 yr BP. The paleoclimate data from the Edwards Plateau for the last 1000 years used for these reconstructions is limited (12), but xeric conditions are generally inferred.

Our paleoclimate reconstruction is consistent with these records in predicting the onset of dry climate at 7320 cal yr BP (6420 yr BP), and a dominant warm period from 5020 to 2840 cal yr BP (4400 to 2730 yr BP). We also agree with a return to wet-cool conditions ~2500 yr BP with a mesic period (M3) from 2840 to 2080 cal yr BP (2730 to 2080 yr BP); however, we indicate a brief xeric period (X2) between 2080 and 1760 cal yr BP (2080 to 1830 yr BP), followed by a return to mesic conditions (M2) from 1760 to 1360 cal yr BP (1830 to 1440 yr BP). These ephemeral wet/dry climate episodes could account of the inconsistency in the earlier reconstructions reported by Bryant and Holloway (11) and Toomey *et al.* (12). We suggest the

former recorded the rapid return to dry conditions (X2), but failed to resolve the ensuing wet period (M2). The later did not resolve X2, resulting in the prediction of an extended wet period. Finally, our paleoclimate reconstruction does not match the dry conditions for the last 1000 years inferred by these authors; instead, we predict conditions of low E:P beginning about 680 cal yr BP (730 yr BP) that persisted until present.

The record of climate change reflected in the oxalate  $^{14}\text{C}$  data also agrees with global climate trends (Fig. 2). For example, the single  $^{14}\text{C}$  age at 7320 cal yr BP corresponds to the onset of the Holocene Climate Optimum (13), and clusters X4 and X3 (from 6380 to 2840 cal yr BP) occur during this period of elevated global temperatures. Although the termination of the Holocene Climate Optimum is generally indicated at ca. 4000 yr BP (13), paleoclimate reconstructions for southwestern Texas (11, 12), as well as records from along or near 100° W meridian in North America (14, 15), indicate that dry conditions continued until ca. 3000 yr BP which is consistent with our record. Other widespread Holocene climate trends include the Medieval Warm Period and the Little Ice Age — we show xeric conditions (X1) from 1360 to 680 cal yr BP (1440 to 730 yr BP) which coincides with the timing of the Medieval Warm Period (MWP), and mesic conditions (M1) beginning 680 cal yr BP (730 yr BP) that continued to present corresponding to the Little Ice Age (LIA). Finally, the timing of xeric/mesic climate changes we interpret for southwestern Texas is remarkably consistent with warm-dry/cool-wet climate fluctuations predicted by Campbell *et al.* (16) based on the combination of periodicities observed in a sediment proxy from Pine Lake and the 23,708 yr Milankovitch periodicity (Fig. 2C).

The reliability of oxalate radiocarbon ages representing wet-dry climate fluctuations is subject to three assumptions: (A) The oxalate was produced only during dry climate conditions; (B) Multiple episodes of oxalate production were distinguished in samples selected for

radiocarbon dating; and (C) Bicarbonate from the substrate was not metabolized by the lichen.

(A) Similarities in the micromorphology and chemistry of the oxalate crust throughout the southern Edwards Plateau (4), as well as the characteristic microenvironment in which it occurs, suggests the biogenic substance was produced by either a single lichen or related species; thus, the first assumption is likely valid. (B) If the second assumption is not true then measurements of oxalate  $^{14}\text{C}$  ages would produce dates that are average ages of two or more periods of oxalate deposition, and would not correspond to climate regimes. We analyzed samples using optical microscopy and SEM in an attempt to exclude such samples in our data base. (C) The last assumption would cause anomalously old  $^{14}\text{C}$  ages due to inclusion of "dead" carbon from the limestone. That this does not occur to a substantial degree is evident in that the  $^{14}\text{C}$  ages are relatively recent; much older dates would be obtained if significant amounts of bicarbonate were incorporated within the oxalate. Furthermore, we removed and radiocarbon dated discrete oxalate strata from samples 41VV129-1 and 41VV128-7 and obtained ages that are conformable. From sample 128-7 we obtained  $^{14}\text{C}$  ages of 3010 and 4670 cal yr BP for top and bottom layers, respectively, and for 41VV129-1 ages of 1970 and 3460 cal yr BP were obtained for the upper and lower layers. Moreover, one of these samples (41VV129-1) contained a layer of prehistoric rock paint produced between 2950 to 4200 yr BP (17) that occurred immediately below the lower oxalate strata dated at 3460 cal yr BP (3220 yr BP), further demonstrating that little if any limestone carbon was metabolized by the lichen.

The oxalate  $\delta^{13}\text{C}_{\text{PDB}}$  values (mean =  $-10.6\text{‰}$ ; range =  $-7.6\text{‰}$ ) indicate an enrichment in  $^{13}\text{C}$  compared to previous reports of  $\delta^{13}\text{C}_{\text{PDB}}$  for lichen thalli, which range from  $-35$  to  $-14\text{‰}$  (18). As we argued above, the primary enrichment in  $^{13}\text{C}$  can not be due to a incorporation of limestone carbon. Instead, we suggest the  $^{13}\text{C}$  enrichment reflects a metabolic shift (19);

however, we can not rule out a minor bicarbonate component in the production of oxalate.

The results of this study demonstrate the potential for obtaining high resolution paleoclimate data from biogenic residues on rock surfaces. Lithobiont communities are common in desert regions (20), and the distribution of these communities are dependent on environmental conditions (21). We suggest that radiocarbon dating of metabolic byproducts of lichen or microbes with specific climate requirements could provide a new source of paleoclimate information. Moreover, the paleoclimate record presented here indicates that southwestern Texas experienced wet-dry climate fluctuations during the mid and late Holocene that followed global climate trends more closely than indicated by previous reconstructions.

#### REFERENCES AND NOTES

---

1. S. R. O'Brien *et al.*, *Science* **270**, 1962 (1995).
2. D. Rind and J. Overpeck, *Quat. Sci. Rev.* **12**, 357.
3. O. K. Davis, *Science* **223**, 617 (1984).
4. J. Russ *et al.*, *Quat. Res.* **46**, 27 (1996).
5. Samples used in this study were collected from between 29°39'–29°50'N and 100°51'–101°35'W.
6. B. Curtiss, J. B. Adams and M. S. Ghiorso, *Geochim. Cosmochim. Acta* **49**, 49 (1985).
7. O. L. Lange and A. T. G. Green, *Oecologia* **108**, 13 (1996).
8. L. Kappen, in *The Lichens*, V. Ahmadjian and M. E. Hale, Eds. (Academic Press, New York, 1973), pp. 311-379.
9. To test whether the type of acid affects the  $^{14}\text{C}$  age, we divided a single sample into four aliquots, two of which were digested in 5% acetic acid and two in dilute phosphoric acid. The

following results demonstrate there is no measurable difference in the  $^{14}\text{C}$  ages:

| <u>Sample No.</u>       | <u>C-14 age (yr BP)</u> | <u>CAMS No.</u> |
|-------------------------|-------------------------|-----------------|
| EN3-a (phosphoric acid) | $1360 \pm 60$           | 29408           |
| EN3-b (phosphoric acid) | $1280 \pm 60$           | 29409           |
| EN3-c (acetic acid)     | $1340 \pm 50$           | 29410           |
| EN3-d (acetic acid)     | $1260 \pm 50$           | 29411           |

Control samples were prepared from solutions of NBS  $^{14}\text{C}$  standard oxalic acid (SRM 4990-C) and calcium chloride hydrate (99.99+%) by mixing the solutions and filtering the calcium oxalate precipitant. Two samples (labeled CaOx 1-S and CaOx 2-S) were processed in the acetic acid solution, washed and dried, while one sample (CaOx 3-S) remained untreated. The three control samples were then processed for radiocarbon analysis. Duplicate analyses of each yielded the following results:

| <u>Sample No.</u> | <u>Fraction modern</u> | <u>CAMS No.</u> |
|-------------------|------------------------|-----------------|
| CaOx 1-S          | $1.3355 \pm 0.0072$    | 14412           |
| CaOx 1-S          | $1.3436 \pm 0.0088$    | 14415           |
| CaOx 2-S          | $1.3446 \pm 0.0087$    | 14413           |
| CaOx 2-S          | $1.3516 \pm 0.0076$    | 14416           |
| CaOx 3-S          | $1.3480 \pm 0.0093$    | 14414           |
| CaOx 3-S          | $1.3374 \pm 0.0132$    | 14417           |

Expected fraction modern = 1.341



10. J. S. Vogel, D. E. Nelson and J. R. Southon, *Radiocarbon* **29**, 323 (1987).
11. V. M. Bryant and R. G. Holloway, in *Pollen Records of Late-Quaternary North American Sediments*, V. M. Bryant and R. G. Holloway, Eds. (Am. Assoc. Stratigr. Palynol., Dallas, 1985) pp. 39-70.
12. R. S. Toomey, M. D. Blum and S. Valastro, *Global and Planetary Change* **7**, 299 (1993).
13. C. K. Folland *et al.*, in *Climate Change. The IPCC Scientific Assessment*, J. T. Houghton, G. J. Jenkins and J. J. Ephraums, Eds. (Cambridge University Press, 1990) pp. 194-238.
14. H. Nichols, in *Arctic and Alpine Environments*, J. D. Ives and R. J. Barry, Eds. (Methuen, London) pp. 637-667.
15. R. G. Baker *et al.*, *Quat. Res.* **37**, 379 (1992).
16. I. D. Campbell *et al.*, *Geology* **26**, 471 (1998).
17. J. Russ *et al.*, *Radiocarbon* **34** 867-872 (1992); W. Ilger, *et al.*, *Radiocarbon* **37** 299-310 (1995).
18. O. L. Lange, T. G. A. Green and H. Ziegler, *Oecologia* **75**, 494 (1988).
19. For higher plants an  $\sim 5\text{‰}$  enrichment of  $^{13}\text{C}$  in plant oxalates with respect to the plant body has been observed. E. R. Rivera and B. N. Smith, *Plant Physiol.* **64**, 966 (1979).
20. J. T. Staley, F. Palmer and J. B. Adams, *Science* **215**, 1093-1094 (1982).
21. A. Danin, *Proceedings of the Royal Society of Edinburgh* **89B**, 243-253 (1986); A. Danin, *Israeli Journal of Earth Science* **41**, 201-207 (1993).
22. We thank J. Labadie, E. Brotherton and J. Skiles for help with field work, R. Palma for helpful discussions, and J. Southon for the AMS dating. Support for this research was provided by a Cottrell Science Award of Research Corporation and a grant from the National Center for Preservation Technology and Training.

| Site and<br>Sample No. | CAMS<br>No. | $^{14}\text{C}$ age <sup>§</sup><br>(yr BP) | $\delta^{13}\text{C}_{\text{PDB}}$<br>(‰) | Calibrated Age <sup>*</sup><br>(cal yr BP) | Calendar Age<br>(AD/BC) |
|------------------------|-------------|---|---|--|-------------------------|
| 41VV89-5B              | 15131       | 730 ± 80                                    | -12.93                                    | 680 ± 80                                   | 1270                    |
| 41VV89-26              | 15130       | 890 ± 60                                    | -13.70                                    | 820 ± 60                                   | 1130                    |
| 41VV89-6A2             | 15134       | 1060 ± 60                                   | —   | 990 ± 60                                   | 960                     |
| 41VV167-3 <sup>†</sup> | (9)         | 1310 ± 30                                   | -10.24                                    | 1240 ± 30                                  | 710                     |
| 41VV89-6A1             | 15133       | 1330 ± 60                                   | —   | 1240 ± 60                                  | 710                     |
| 41VV167-1A             | 31153       | 1440 ± 60                                   | —   | 1360 ± 50                                  | 590                     |
| 41VV75-1               | 15132       | 1830 ± 70                                   | —   | 1760 ± 80                                  | <u>190 AD</u>           |
| 41VV129-1A (T)         | 15146       | 2000 ± 80                                   | -6.08                                     | 1970 ± 100                                 | 20 BC                   |
| 41VV83-1*              | *           | 2080 ± 90                                   | —   | 2080 ± 120                                 | 130                     |
| 41VV167-1B             | 31154       | 2080 ± 60                                   | -9.7                                      | 2070 ± 90                                  | 120                     |
| 41VV123-10             | 15135       | 2730 ± 50                                   | -8.3                                      | 2840 ± 50                                  | 890                     |
| 41VV128-7B (T)         | 15143       | 2860 ± 80                                   | -7.59                                     | 3010 ± 110                                 | 1060                    |
| Pecos WB-2             | 31156       | 2860 ± 80                                   | -11.1                                     | 3010 ± 110                                 | 1060                    |
| 41VV576-Ac             | 15145       | 3020 ± 70                                   | -9.85                                     | 3220 ± 100                                 | 1270                    |
| 41VV129-1B (B)         | 15147       | 3220 ± 60                                   | -9.2                                      | 3460 ± 70                                  | 1510                    |
| Skiles-2               | 31155       | 3400 ± 60                                   | -11.6                                     | 3670 ± 90                                  | 1720                    |
| 41VV165-1A             | 31162       | 3500 ± 60                                   | -11.7                                     | 3790 ± 80                                  | 1840                    |
| Pressa4-1A             | 31157       | 3750 ± 60                                   | -11.6                                     | 4140 ± 100                                 | 2190                    |
| 41VV90-1               | 11437       | 3990 ± 60                                   | -9.5                                      | 4500 ± 110                                 | 2550                    |
| 41VV128-7D (B)         | 15144       | 4130 ± 60                                   | —   | 4670 ± 100                                 | 2720                    |
| Pressa4-1A             | 31159       | 4400 ± 60                                   | -11.6                                     | 5020 ± 120                                 | 3070                    |
| Pressa4-3A             | 31160       | 5230 ± 50                                   | -11.6                                     | 6030 ± 80                                  | 4080                    |
| Pressa4-3B             | 31161       | 5290 ± 60                                   | -11.4                                     | 6080 ± 80                                  | 4130                    |
| 41VV888-1              | 11438       | 5570 ± 60                                   | —   | 6380 ± 60                                  | 4430                    |
| Pressa4-1B             | 31158       | 6420 ± 60                                   | -12.4                                     | 7320 ± 70                                  | 5370                    |

<sup>§</sup> The measured  $\delta^{13}\text{C}_{\text{PDB}}$  was used for calculating the  $^{14}\text{C}$  age when available; otherwise, the average  $\delta^{13}\text{C}_{\text{PDB}}$  value (-10.5 ‰) was used for the calculation.

<sup>\*</sup> Calculated using Calibeth Version 1.5 ETH Zurich (Swiss Federal Institute of Technology).

<sup>†</sup> Represents an average of 4 aliquots, two digested in 5% double distilled acetic acid and two digested in dilute phosphoric acid (9).

• Datum is an average of 3 aliquots (2070 ± 50, 2080 ± 50 and 2100 ± 50, with CAMS Nos. 11145, 11146 and 11147, respectively)

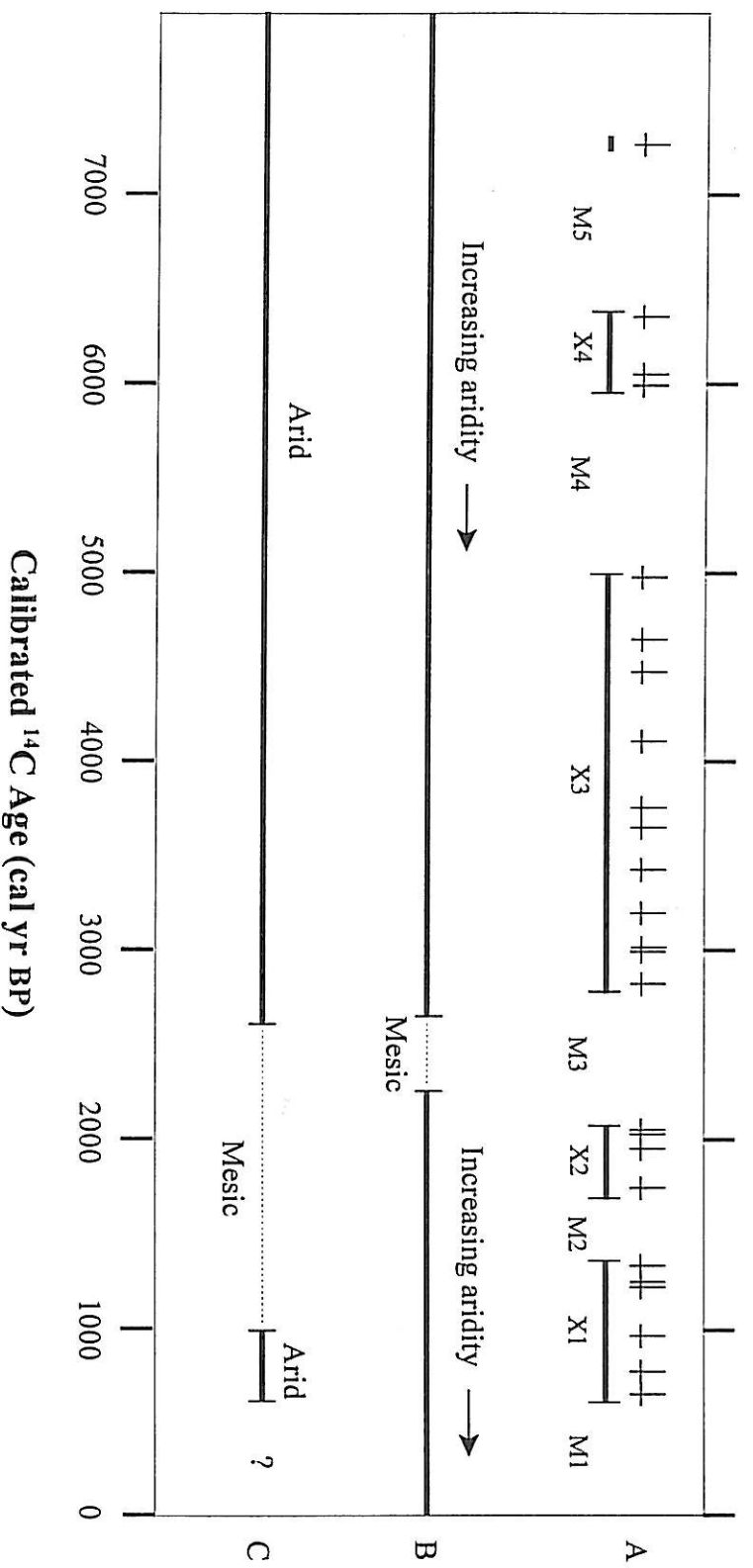


Fig. 1. (A) Temporal distribution of calibrated  $^{14}\text{C}$  ages (cal yr BP) of calcium oxalate residues from the southern Edwards Plateau. We propose that clusters of radiocarbon ages indicate periods of high E:P, while gaps in the data correspond to periods with low E:P. We show four xeric episodes (X1–X4), punctuated by five mesic episodes (M1–M5). Also shown are paleoclimate reconstructions by (B) Bryant and Holloway (11) based on palynological data and (C) Toomey *et al.* (12) based on palynological, plant macrofossil, and vertebrate fossil data. Solid lines show arid periods, while dotted lines indicate mesic intervals. Arrows in B indicate periods of increasing aridity.

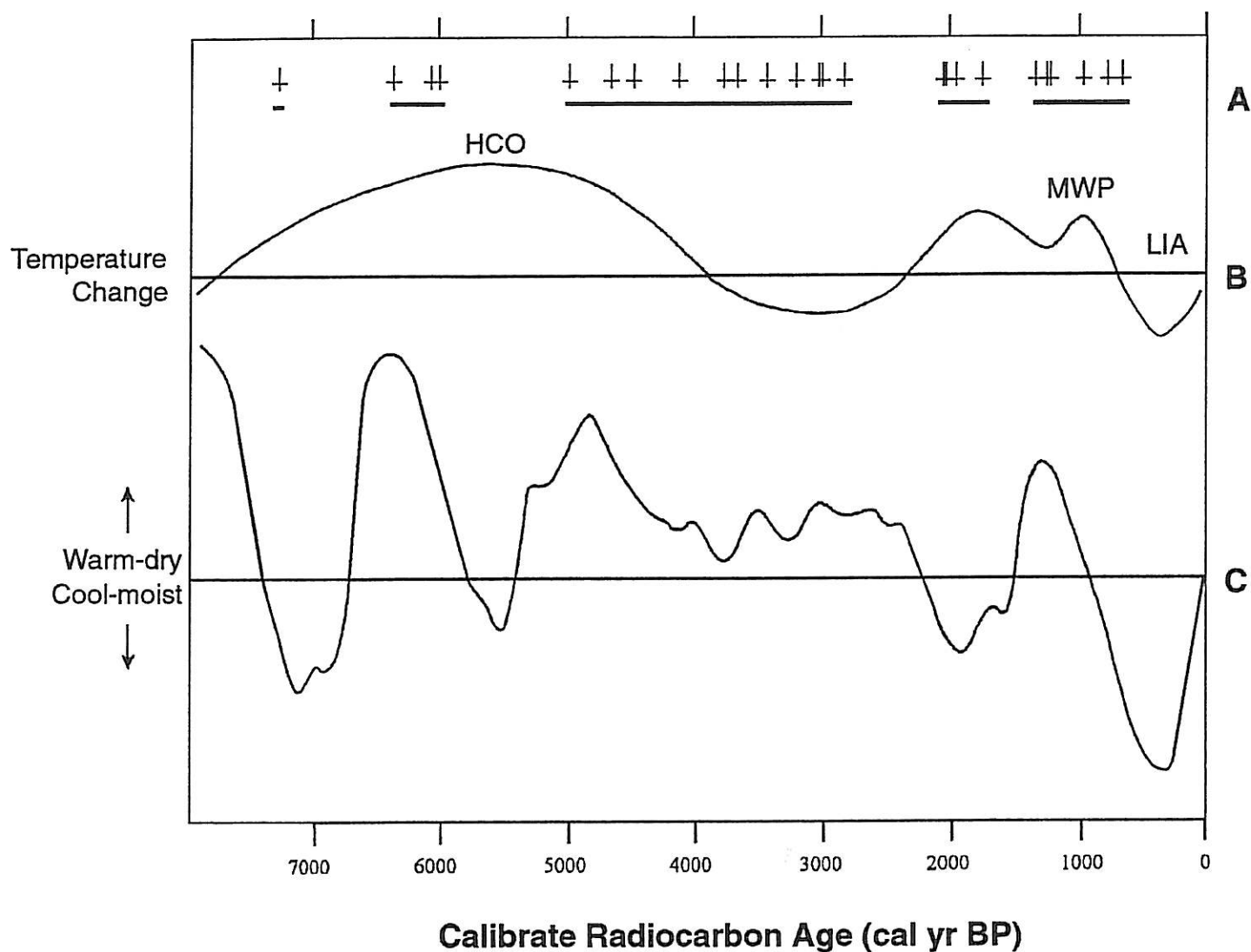


Fig. 2. (A) paleoclimate reconstruction presented here showing comparisons with global climate trends, including the Little Ice Age (LIA), the Medieval Warm Period (MWP), and the Holocene Climate Optimum (HCO). (B) Variations in the global mean temperature (GMT) relative to the GMT near the beginning of the 20<sup>th</sup> century (modified from 13). (C) Cool-moist/warm-dry climate variations relative to current conditions as proposed by Campbell *et al.* (15) based on calculated periodicities observed in a sediment proxy from Pine Lake (52°04'N, 113°27'W) and the 23,708 yr Milankovitch periodicity (adapted from 15).

## Table and Figure captions

Table 1. Radiocarbon ages and  $\delta^{13}\text{C}_{\text{PDB}}$  values of oxalate rock crusts. Sample numbers with 41VV- prefixes refer to archaeological sites, while those with names (Skiles, Pressa, and Pecos) refer to sites that are not archaeological. The parenthesized letters in the first column refer to upper (T) and lower (B) strata from samples that showed two oxalate layers that were removed and analyzed separately.

Fig. 1. (A) Temporal distribution of calibrated  $^{14}\text{C}$  ages (cal yr BP) of calcium oxalate residues from the southern Edwards Plateau. We propose that clusters of radiocarbon ages indicate periods of high E:P, while gaps in the data correspond to periods with low E:P. We show four xeric episodes (X1–X4), punctuated by five mesic episodes (M1–M5). Also shown are paleoclimate reconstructions by (B) Bryant and Holloway (11) based on palynological data and (C) Toomey *et al.* (12) based on palynological, plant macrofossil, and vertebrate fossil data. Solid lines show arid periods, while dotted lines indicate mesic intervals. Arrows in B indicate periods of increasing aridity.

Fig. 2. (A) paleoclimate reconstruction presented here showing comparisons with global climate trends, including the Little Ice Age (LIA), the Medieval Warm Period (MWP), and the Holocene Climate Optimum (HCO). (B) Variations in the global mean temperature (GMT) relative to the GMT near the beginning of the 20<sup>th</sup> century (modified from 13). (C) Cool-moist/warm-dry climate variations relative to current conditions as proposed by Campbell *et al.* (15) based on calculated periodicities observed in a sediment proxy from Pine Lake (52°04'N, 113°27'W) and the 23,708 yr Milankovitch periodicity (adapted from 15).